

Contribution of an asphalt pavement modified with TiO_2 to the moderation of the Urban Heat Island (UHI)

Pablo Cabrera ^a, Gerardo Botasso ^a & Ana M. Castro-Luna ^{a, b}

^a Universidad Tecnológica Nacional, Facultad Regional La Plata, LEMaC Centro de Investigaciones Viales UTN FRLP - CIC PBA, La Plata, Buenos Aires, Argentina. pcabrera@frlp.utn.edu.ar, gerardobot@hotmail.com

^b Comisión de Investigaciones Científicas de la Provincia de Buenos Aires CIC PBA, La Plata, Argentina. castrolu@gmail.com

Received: March 25th, 2025. Received in revised form: May 5th, 2025. Accepted: May 16th, 2025

Abstract

Urban pavements, covering up to 40% of cities, intensify the Urban Heat Island (UHI) phenomenon by impeding rainwater infiltration and absorbing solar radiation. High pavement temperatures increase urban energy demand and pollution. One important factor affecting pavement temperature is albedo. The higher the albedo, the less solar irradiation the pavement absorbs, and the cooler it remains. This study evaluates TiO_2 incorporated into asphalt to enhance albedo. The thermal response of conventional and TiO_2 -modified pavements was monitored under natural sunlight. Opto-thermal properties were measured initially and after twelve months of outdoor exposure. An energy balance quantified the heat amount released to the environment for both pavements. Results demonstrate TiO_2 effectiveness in reducing heat storage and improving radiative cooling over time. Additionally, the mechanical and rheological impacts of TiO_2 on asphalt binders were analyzed. Cool pavements with TiO_2 emerge as a viable UHI mitigation strategy, offering energy savings and enhanced urban sustainability.

Keywords: modified asphalt pavements; TiO_2 ; urban heat island; albedo; aging; released energy.

Contribución de un pavimento asfáltico modificado con TiO_2 a la moderación de la Isla de Calor Urbana (ICU)

Resumen

Los pavimentos urbanos, que cubren hasta el 40% de las ciudades, intensifican el fenómeno de la Isla de Calor Urbana (ICU) al impedir la infiltración de agua de lluvia y absorber la radiación solar. Las altas temperaturas del pavimento aumentan la demanda energética urbana y la contaminación. Un factor importante que afecta la temperatura del pavimento es el albedo. Cuanto mayor es el albedo, menor es la radiación solar que absorbe el pavimento y más frío se mantiene. Este estudio evalúa el TiO_2 incorporado al asfalto para mejorar el albedo. Se monitoreó la respuesta térmica de los pavimentos convencionales y modificados con TiO_2 bajo la luz solar natural. Se midieron las propiedades opto-térmicas inicialmente y después de doce meses de exposición al aire libre. Un balance energético cuantificó la cantidad de calor liberado al ambiente para ambos pavimentos. Los resultados demuestran la eficacia del TiO_2 para reducir el almacenamiento de calor y mejorar el enfriamiento radiativo con el tiempo. Además, se analizaron los impactos mecánicos y reológicos del TiO_2 en los ligantes asfálticos. Los pavimentos fríos con TiO_2 surgen como una estrategia viable de mitigación de UHI, que ofrece ahorros de energía y una mayor sostenibilidad urbana.

Palabras clave: pavimentos de asfalto modificados; TiO_2 ; isla de calor urbana; albedo; microclima.

1. Introduction

In recent decades, large-scale production of goods and industrial activities have caused an increase in the number of

residents living in cities near production centers. The population density in cities is continuously growing and it is estimated that by 2050, nearly 70% of the world's population will live in megacities.

How to cite: Cabrera, P., Botasso, G., and Castro-Luna, A.M., Contribution of an asphalt pavement modified with TiO_2 to the moderation of the Urban Heat Island (UHI). DYNA, 92(237), pp. 80-88, April - June, 2025.

To accommodate this ever-growing urban population, a housing and communication infrastructure that causes significant environmental changes has been implemented: there is an increasing replacement of natural soil with impermeable soil, and materials with inadequate optothermal properties are used in construction [1,2].

At present, almost half of urban land has been replaced by asphalt pavement. During the day, due to the incidence of solar irradiation, these pavements heat up and afterward release heat to the environment. Asphalt pavements are dark, so as a black body, they absorb a significant portion of the incident solar irradiation as heat, reaching surface temperatures close to 70°C in some geographic regions during the summer. Higher pavement surface temperatures are one of the causes of the urban heat island effect, UHI, with air temperatures higher in the city than in the surrounding suburbs and rural areas [3].

A conventional asphalt pavement transfers heat to its interior, stores it during sunlight hours, and releases it into the air during the evening and night hours, causing thermal discomfort for city dwellers [4-9].

There is a huge consumption of fossil energy to cool premises and residences and air pollution occurs in large cities. In addition, due to the viscoelastic nature of asphalt, the load resistance of the pavement decreases as the temperature increases and rutting occurs on the surface, reducing the service life of the pavement. During the life of the pavement, changes occur in the composition of the asphalt binder. The laboratory-aging test reveals that the asphalt became stiffer and more prone to cracking by losing its viscous component due to temperature, humidity and the incidence of the ultraviolet (UV) component of solar radiation, among other environmental factors to which an outdoor pavement is subjected. The pavement undergoes modifications in its structure and cracks and rut appear on the surface [10-13]. Many studies have identified permanent deformation induced by high temperatures as one of the main problems in asphalt pavements in the current climate change situation.

To mitigate the UHI (Urban Heat Island) effect, among other possible solutions, it is recommended to use paving materials with higher albedo, which is defined as the ratio between reflected solar irradiation and the total solar irradiation incident on the surface [3]. The higher the albedo value is, the less solar irradiation the pavement absorbs, and the cooler it remains. The most common comparison between asphalt and concrete pavements shows that the latter has a cooler surface due to its lighter color [4,14]. Various strategies have been proposed to reduce the amount of heat absorbed and stored by pavement, including the incorporation of pigments into asphalt mixtures to achieve a lighter surface color, particularly on the top layer [15]. Chen et al. affirm that incorporating TiO₂ fillers at varying percentages into a transparent resin, which is subsequently applied as a coating on different asphalt mixtures, significantly enhances the albedo value, depending on the size and concentration of the fillers [16].

Zhong has demonstrated that modifying an asphalt emulsion with varying percentages of TiO₂ and applying it as a surface coating reduces the pavement's surface temperature by approximately 5°C [17]. Cool pavements can be

implemented in urban areas as a strategy to mitigate the adverse effects of urban heat islands. By preventing pavement overheating, energy savings are achieved, and the urban microclimate is improved.

It is noteworthy that asphalt pavements, initially dark in color, lighten over time, slightly increasing their albedo and reducing heat absorption as they age in service. This outdoor color variation is attributed to irreversible physicochemical modifications of the asphalt (aging), caused by a complex oxidation process of its organic compounds under the influence of environmental factors such as rainfall, temperature fluctuations, and UV component of incident solar irradiation, which photo-catalyzes the degradation [11].

This study analyzes the optothermal response of dense asphalt pavement specimens, before and after the incorporation of TiO₂ microparticles (average size 0.5 µm) as fillers in the asphalt mixture.

The surface temperature, albedo, and emissivity of the exposed samples were measured, and the effect of prolonged outdoor exposure on their thermal behavior was evaluated. Additionally, using an energy balance approach, the heat released by the samples into the environment was calculated both initially and after 12 months of outdoor exposure. The effect of TiO₂ microparticles on the physical properties of asphalt, high-temperature performance grade, and fatigue damage tolerance were also investigated using a dynamic shear rheometer (DSR).

2. Experimental

Two representative types of dense-graded asphalt mixtures were prepared. The first type utilized an asphalt binder CA-30, stone aggregates with commercial designations of 6:12 (coarse aggregate) and 0:6 (fine aggregate), and combined fillers (lime + all particles smaller than the #200 sieve from the coarse and fine aggregates). This mixture was used to fabricate reference specimens. The second asphalt mixture was prepared by removing the combined fillers, and incorporating 5% of TiO₂, a powdered pigment that meets the specifications of ASTM C979. The TiO₂-modified specimens analyzed in this study were fabricated with this modified asphalt mixture. All specimens were 0.3 m × 0.3 m × 0.05 m. In this paper 'specimen' denote asphalt pavement mixture, and 'sample' denote asphalt binder.

Thermal measurements were conducted by placing the specimens on a polystyrene foam (EPS) sheet 0.1 m thick, which exhibits negligible thermal conductivity (ca. 0.032 W.m-1K-1).

The albedo value of each specimen (reference and TiO₂-modified) was measured following the ASTM E1918A standard modified by Akbari et al. [18], during clear-sky days in January 2024 and January 2025, on the rooftop of the Universidad Tecnológica Nacional, Facultad Regional La Plata (National Technological University, La Plata Regional Faculty). The instrumentation included a calibrated Kipp & Zonen CMP-3 pyranometer coupled to a Campbell Scientific CR300 datalogger.

The thermal behavior of samples exposed to direct solar irradiation was evaluated using K-type thermocouples connected to Testo data-loggers. The surface temperatures of the specimens were recorded continuously every ten seconds over five consecutive days in January 2024, with the measurements repeated under similar conditions in January 2025.

Additionally, a Testo 865 thermal imaging camera was employed to estimate the emissivity (ϵ) of each sample, following the guidelines outlined in ASTM E1933-99a [19]. The camera, with an infrared resolution of 320×240 pixels and a thermal sensitivity of 0.1°C , also enabled visual analysis of surface temperature differences between the samples, complementing the data recorded by the thermocouples.

A simplified model was employed accounting for the heat fluxes occurring between the pavement and its surrounding environment, incorporating the primary energy transfer mechanisms. The model includes: the incident solar irradiation, the portion of it absorbed by the pavement, the heat transferred to the pavement by thermal conduction, the energy released to the environment by convection (sensible heat), and the longwave radiation emitted from the hot pavement surface to the air. Using this framework, the total energy released to the environment by the two types of asphalt pavement was quantified.

To analyze the influence of TiO_2 microparticles on the asphalt binder, physical properties such as penetration (ASTM D5/D5M) [20] and softening point (ASTM D36/D36M) [21] were determined. Additionally, the high and intermediate temperature performance grades (AASHTO M320) [22] were evaluated using a dynamic shear rheometer.

The effect of TiO_2 on the physical and rheological properties of the asphalt binder was evaluated before and after subjecting the samples to thin-film oven aging (RTFOT) following AASHTO T240 [23].

3. Results

3.1 Color variation of asphalt mixtures under outdoor exposure

Fig. 1 shows images depicting the color of reference and 5% TiO_2 -modified asphalt pavement specimens, both initially and after one year of outdoor exposure.

Initially, the reference specimen exhibits a characteristic black color, whereas the TiO_2 -modified specimen displays a

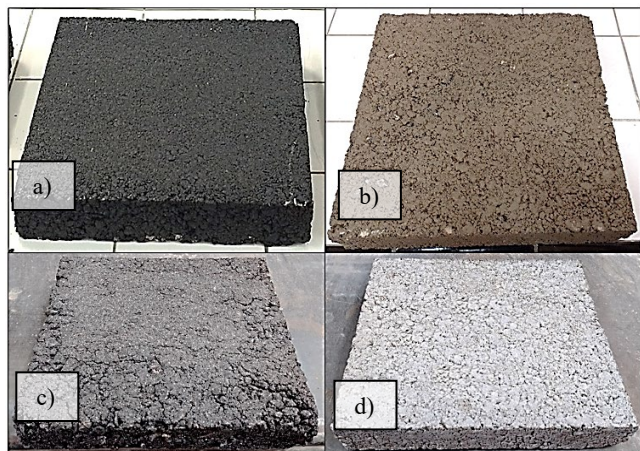


Figure 1. Images of the samples: a) reference asphalt pavement and b) TiO_2 -modified asphalt pavement, at month 1; c) reference asphalt pavement and d) TiO_2 -modified asphalt pavement, after 12 months of outdoor exposure. Source: Authors' own work.

brown coloration [27]. This suggests that TiO_2 may have catalyzed a chemical transformation in the asphalt from the beginning of the experiment [24-25]. After 12 months of outdoor exposure, the reference specimen developed a dark gray coloration, while the TiO_2 -modified sample exhibited a light gray tone. It can be concluded that prolonged outdoor exposure has caused surface color variations in both analyzed samples.

The observed color change in both specimens is attributed to the oxidation process of the asphalt due to a prolonged stay in open air (UV radiation, rainfall, oxygen, etc), a process catalyzed by TiO_2 in the modified specimen [26].

A cross-sectional cut was performed on the reference and TiO_2 -modified samples exposed to outdoor conditions for 12 months to determine whether the color change was superficial or occurred throughout the whole specimen's volume. Fig. 2 shows images of the cross-sectional cuts of the (a) reference and (b) TiO_2 -modified specimens. In both cases, a color difference is observed between the air-exposed surface and the sample's interior, which can be attributed to a greater aging of the surface due to UV radiation exposure. The cross-section of the TiO_2 -modified specimen exhibits a marked color difference between the surface and the interior of the modified asphalt mixture. It is possible that the presence of TiO_2 catalyzes the reaction between asphalt and oxygen under UV radiation, resulting in a noticeable surface color change in the TiO_2 -modified sample compared to the surface color change observed in the reference specimen for the same reaction.

3.2 Albedo values determined at solar noon on a summer day

The variation in albedo of the pavement specimens before and after being exposed to outdoor conditions for 12 months is shown in Fig. 3. The albedo measurement of each specimen was repeated six times and the standard deviation obtained was $\pm 0.3\%$.

It is confirmed that the incorporation of TiO_2 into the asphalt mixture increased the albedo at the start of the experiment.



Figure 2. Cross-sectional cut in a) the reference specimen and b) the TiO_2 -modified specimen exposed to outdoor conditions for 12 months. Source: Authors' own work.

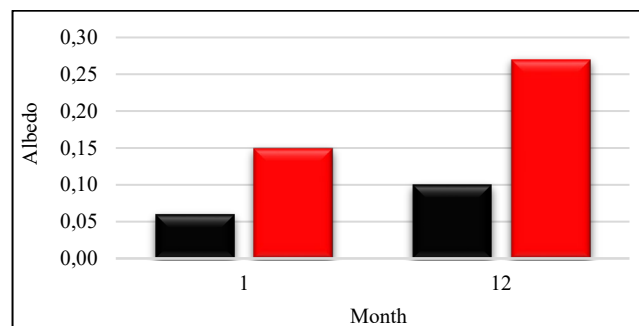


Figure 3. Albedo values for reference specimen (black) and TiO_2 -modified specimen (red) at month 1 and after 12 months of outdoor exposure. Source: Authors' own work.

After 12 months of outdoor exposure, both pavements exhibit an increase in their albedo values, with the TiO₂-modified specimen showing a particularly significant rise. An increase in albedo implies a lower surface temperature of the asphalt pavement exposed to solar irradiation [28-29].

3.3 Variation in surface temperature of samples exposed to outdoor conditions

Figs. 4a and 4b illustrate the surface temperature variations of the reference and TiO₂-modified asphalt pavement specimens over a five-day period a) at the start of outdoor exposure and b) after 12 months of outdoor exposure.

Fig. 4a shows that, at the start of outdoor exposure, the TiO₂-modified asphalt pavement specimen exhibits a decrease of approximately 4°C in its surface temperature value particularly when the Sun is at its zenith. After 12 months of outdoor exposure, Fig. 4b reveals that the TiO₂-modified sample displays a more pronounced decrease in surface temperature, approximately 10°C, compared to the value recorded in the reference sample, especially during solar zenith. The observed decrease in temperature correlates with the higher albedo values measured in the specimen after 12 months of outdoor exposure. Similar behavior of the pavement superficial temperature during the solar day has been shown in [17].

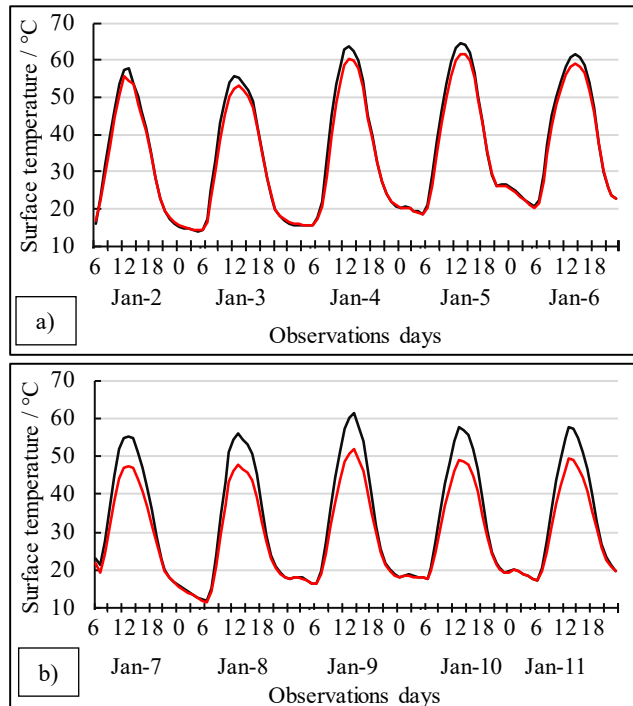


Figure 4. Surface temperature variation over five studied days, due to daily solar irradiation on the reference asphalt pavement specimen (black line) and on the TiO₂-modified pavement specimen (red line): a) at month 1 and b) after 12 months of outdoor exposure.

Source: Authors' own work.

3.4 Thermographic Images

The change in surface temperature of the analyzed specimens can be qualitatively observed in the thermographic images shown in Fig. 5. The color scale illustrates that both samples (reference and TiO₂-modified asphalt pavement) at the start and after one year of outdoor exposure, exhibit lower surface temperatures, with this cooling effect being more pronounced in the TiO₂-modified specimen.

Using thermographic images and data recorded with thermocouples, the emissivity (ϵ) of each analyzed surface was determined. The emissivity values (ϵ), both at month 1 and month 12, were 0.91 for the reference specimen and 0.97 for the TiO₂-modified specimen.

3.5 Variation of Heat Released to the Environment for Each Analyzed Pavement

The thermal balance of a pavement exposed to solar irradiation must account for:

- The amount of solar irradiation absorbed by the pavement,
- The heat flux transferred by conduction (Q_{cond}) into the pavement's interior,
- The infrared radiation (Q_{rad}) emitted by the surface of the heated body,
- The heat flux, transferred by convection (Q_{conv}), from the hot surface to the air.

According to the Bentz model [30] and following the analyses by Asaeda [31] Qin et al and Xu et al. [32,33], the energy balance at the surface of a dry pavement is:

$$I \cdot (1 - \text{albedo}) = h_c \cdot (T_s - T_{\text{amb}}) + \epsilon \cdot \sigma \cdot (T_s^4 - T_c^4) - k \cdot (dT/dz) \quad (1)$$

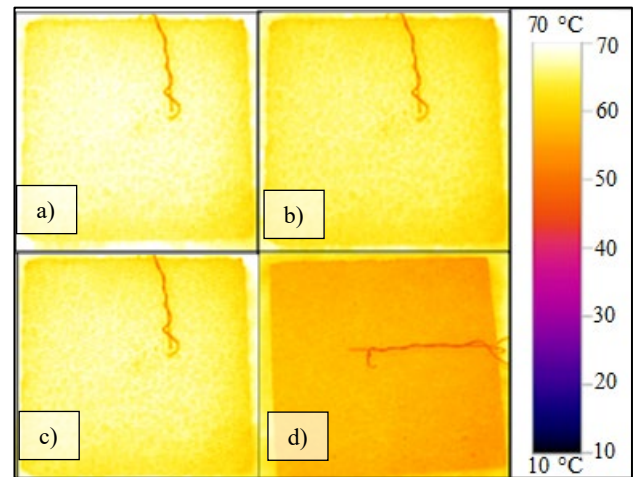


Figure 5. Thermal images of specimens exposed to outdoor conditions: a) and b) reference asphalt pavement and TiO₂-modified asphalt pavement at month 1, respectively; c) and d) reference asphalt pavement and TiO₂-modified asphalt pavement after 12 months of outdoor exposure, respectively.

Source: Authors' own work.

where I is the incident solar irradiation on the sample surfaces; h_c [$\text{W}\cdot\text{m}^{-2}\cdot\text{K}^{-1}$] is the convective coefficient, dependent on wind speed; T_s [K] is the pavement surface temperature; T_{amb} is the ambient temperature [K]; σ is the Stefan-Boltzmann constant (5.67×10^{-8} [$\text{W}\cdot\text{m}^{-2}\cdot\text{K}^{-4}$]); ε is the emissivity of the pavement (dimensionless, ranging between 0 and 1); T_c [K] is the sky temperature; k [$\text{W}\cdot\text{m}^{-1}\cdot\text{K}^{-1}$] is the material's thermal conductivity; and dT/dz [$\text{K}\cdot\text{m}^{-1}$] is the thermal gradient into the pavement's interior.

The portion of solar energy that is not reflected by the surface is absorbed by the pavement. The absorbed energy is partially transferred throughout the pavement's volume via conduction, increasing its temperature. Additionally, a heated body emits radiation in the infrared (IR) region of the electromagnetic spectrum. This radiative heat transfer depends on the surface temperature value and the emissivity of the composite material. Furthermore, when the pavement's surface temperature exceeds the temperature of the air above it, part of the absorbed energy begins to be transferred from the pavement surface to the air via convection (sensible heat). Convective heat transfer to the environment depends on the surface temperature of the heated sample, the surrounding air temperature, and the wind speed over the analyzed surface.

Using the surface temperature data shown in Fig. 4a and 4b, considering the thermal balance, and accounting for the variation in the optical properties that the samples undergo after being exposed to the outdoors for 12 months, the energy released into the environment as sensible heat and longwave radiation is calculated over a five-day period using eq (1).

Fig. 6 shows the behavior of each component of the energy balance (at month 1 and after 12 months) for the reference sample and the TiO₂-modified sample of outdoor exposure, both over five consecutive days.

It is confirmed that the TiO₂-modified sample absorbs less energy than the reference sample, which is directly reflected in the amount of energy the sample releases to the air adjacent to the surface. This effect is more pronounced when the samples have been exposed to outdoor conditions for 12 months. The amounts of energy flux released to the environment by the samples over the five studied days during both daytime and nighttime periods were calculated.

Table 1 presents the energy flux released to the environment (Q_{rel}) between 06:00 and 20:00 hours, calculated as the sum of sensible and radiative heat, for reference and the TiO₂-modified samples, both over the five studied days, at month 1 and after 12 months of exposure to outdoor conditions.

Table 1 demonstrates that, during daytime hours, the majority of energy flux released to the environment by both specimens occurs as sensible heat (Q_{conv}), with the reference sample exhibiting a higher Q_{conv} value than the TiO₂-modified specimen.

In contrast, during nighttime (Table 2), the total amount of energy released is lower than the one released during the daytime, and it is primarily attributed to long-wave radiation, Q_{rad} , the lower emission value is again for the TiO₂-modified specimen.

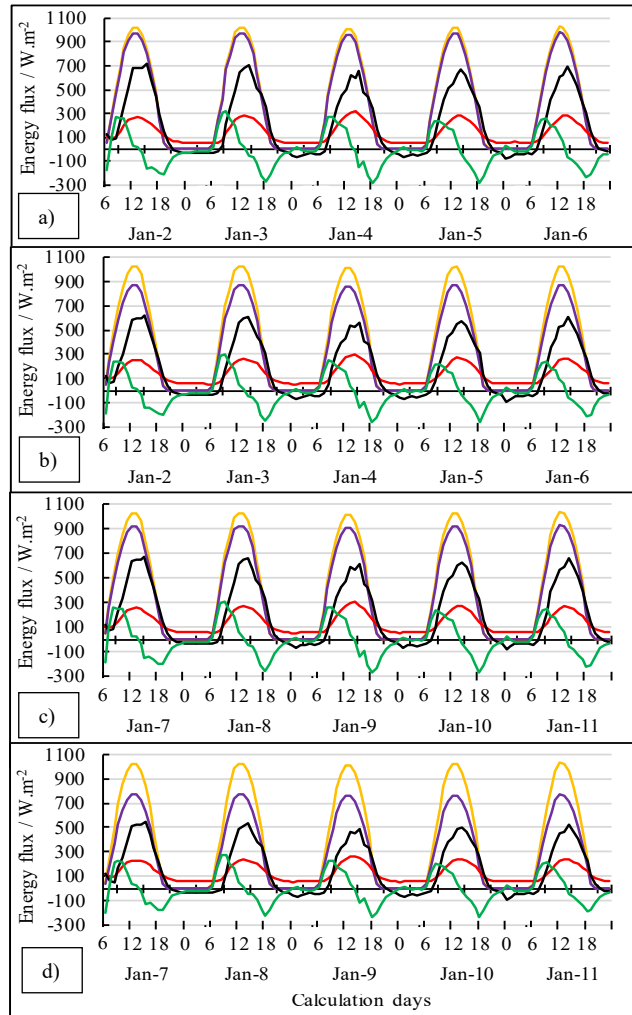


Figure 6. Energy flux components calculated over five days period of: a) reference specimen and b) TiO₂-modified specimen with optical properties of month 1; c) reference asphalt specimen and d) TiO₂-modified asphalt specimen with optical properties of month 12. Lines: yellow: incident solar irradiation; purple: absorbed solar energy; black: energy transferred to the environment via convection; green: long-wave IR energy emitted to the environment; red: heat flux between the pavement surface and its interior. Source: Authors' own work.

Table 1.

Energy flux released to the environment (Q_{rel}) over the five studied days, by the reference and TiO₂-modified asphalt pavement specimens, between 06:00 and 20:00 hours, before and after 12 months of outdoor exposure.

Month	Reference Specimen		TiO ₂ Modified Specimen	
	$Q_{\text{rel}} / \text{Wh}\cdot\text{m}^{-2}$		$Q_{\text{rel}} / \text{Wh}\cdot\text{m}^{-2}$	
1	$Q_{\text{rad}} / \text{Wh}\cdot\text{m}^{-2}$	$Q_{\text{conv}} / \text{Wh}\cdot\text{m}^{-2}$	$Q_{\text{rad}} / \text{Wh}\cdot\text{m}^{-2}$	$Q_{\text{conv}} / \text{Wh}\cdot\text{m}^{-2}$
	12008.8	26443.4	11503.5	22807.3
	38452.2		34310.9	
	$Q_{\text{rel}} / \text{Wh}\cdot\text{m}^{-2}$		$Q_{\text{rel}} / \text{Wh}\cdot\text{m}^{-2}$	
12	$Q_{\text{rad}} / \text{Wh}\cdot\text{m}^{-2}$	$Q_{\text{conv}} / \text{Wh}\cdot\text{m}^{-2}$	$Q_{\text{rad}} / \text{Wh}\cdot\text{m}^{-2}$	$Q_{\text{conv}} / \text{Wh}\cdot\text{m}^{-2}$
	11483.1	24889.1	10430.7	19718.4
	36372.2		30149.1	
	$Q_{\text{rel}} / \text{Wh}\cdot\text{m}^{-2}$		$Q_{\text{rel}} / \text{Wh}\cdot\text{m}^{-2}$	

Source: Authors' own work.

¹ The sky temperature, T_c , is the average temperature derived from the ground surface under study and the temperature in the upper troposphere, where water vapor content is minimal.

Table 2.

Energy flux released to the environment (Q_{rel}) by the reference and TiO_2 -modified asphalt pavement specimens, over the five studied days, between 20:00 and 06:00 hours, before and after 12 months of outdoor exposure.

Month	Reference Specimen		TiO_2 Modified Specimen	
	$Q_{rel} / Wh.m^{-2}$		$Q_{rel} / Wh.m^{-2}$	
1	$Q_{rad} / Wh.m^{-2}$	$Q_{conv} / Wh.m^{-2}$	$Q_{rad} / Wh.m^{-2}$	$Q_{conv} / Wh.m^{-2}$
	2859.2	-740.7	2978.2	-958.5
	2118.5		2019.8	
12	$Q_{rel} / Wh.m^{-2}$		$Q_{rel} / Wh.m^{-2}$	
	$Q_{rad} / Wh.m^{-2}$	$Q_{conv} / Wh.m^{-2}$	$Q_{rad} / Wh.m^{-2}$	$Q_{conv} / Wh.m^{-2}$
	2848.9	-773.4	2957.1	-1021.1
	2075.5		1936.1	

Source: Authors' own work.

In contrast, during nighttime (Table 2), the total amount of energy released is lower than the one released during the daytime, and it is primarily attributed to long-wave radiation, Q_{rad} , the lower emission value is again for the TiO_2 -modified specimen.

It is observed that the greatest energy flux released from the samples to the environment occurs during the sunlight period. Notably, when comparing the TiO_2 -modified sample energy flux released with that of the reference sample, it is noticed a reduction in the energy flux transferred to the environment by the TiO_2 -modified sample, both initially and after 12 months of outdoor exposure. The TiO_2 -modified pavement, being lighter in color, absorbs less solar heat and lowers its surface temperature, thereby contributing to an improved urban microclimate [5,7].

3.6 Influence of TiO_2 on the physical properties of asphalt CA-30

The effect of TiO_2 on the physical properties of the asphalt binder was evaluated before (virgin) and after subjecting the samples to thin-film oven aging (aged) (RTFOT) following AASHTO T240.

In Table 3, the penetration and softening point values before and after subjecting the samples to thin-film oven aging (RTFOT): i) asphalt CA-30, ii) asphalt CA-30 + combined fillers, and iii) asphalt CA-30 + TiO_2 filler, at the proportions used in the mixture.

Table 3 shows that asphalt with combined fillers has the lowest penetration value and the highest softening point, a

Table 3.

Properties of asphalt CA-30 and fillers modified asphalt CA-30 before and after subjecting the samples to thin-film oven aging (RTFOT).

Samples	Properties	
	Penetration	Softening Point
Virgin asphalt	$46 \times 10^{-1} \text{ mm}$	54 °C
Aged asphalt (RTFOT)	$29 \times 10^{-1} \text{ mm}$	59 °C
Virgin Asphalt + combined fillers	$20 \times 10^{-1} \text{ mm}$	63 °C
Aged Asphalt + combined fillers (RTFOT)	$15 \times 10^{-1} \text{ mm}$	68 °C
Virgin Asphalt + TiO_2 filler	$27 \times 10^{-1} \text{ mm}$	60 °C
Aged Asphalt + TiO_2 filler (RTFOT)	$17 \times 10^{-1} \text{ mm}$	65 °C

Source: Authors' own work.

behavior like to that of asphalt with only TiO_2 as a filler, both, before and after aging. This behavior derives from the filler/asphalt weight ratios, being 1.1 for CA-30 asphalt with combined fillers and 1 for CA-30 with TiO_2 filler.

This indicates that asphalts with fillers (combined or with only TiO_2) have low thermal susceptibility, and therefore, in both cases, the viscosity resists creep changes with increasing temperature [34,35].

3.7 High-Temperature Performance Grade (PG)

To evaluate the high-temperature performance grade of the analyzed asphalt binder (virgin and RTFO-aged) according to AASHTO M320, the rutting parameter ($G^*/\sin\delta$) was determined for asphalt CA-30, asphalt CA-30 + combined fillers, and asphalt CA-30 + TiO_2 filler. Here, G^* (complex modulus) represents a measure of the material's dynamic mechanical properties, and δ (phase angle) corresponds to a measure of its elastic and viscous properties [36,37].

From the $G^*/\sin\delta$ vs. temperature relationship, it was determined that by incorporating TiO_2 into CA-30 asphalt, the rutting failure temperature changed from 64°C for CA-30 asphalt to 76°C for CA-30 asphalt + TiO_2 filler, and 82°C for CA-30 asphalt + combined fillers.

The data reveals an improved performance grade in the asphalt CA-30 modified with combined fillers concerning rutting resistance ($G^*/\sin\delta$) compared to the sample asphalt CA-30 + TiO_2 filler.

However, regarding surface temperatures recorded in specimens shown in Fig. 4a, a contrasting performance is noticed: the TiO_2 -modified specimen exhibits higher albedo, which reduces its surface temperature under the same solar irradiation conditions as those experimented by the reference specimen.

This behavior suggests that, under real-world exposure conditions, the sample prepared with CA-30 asphalt + TiO_2 filler could compensate for its lower intrinsic rutting resistance through its enhanced heat-reflective capacity. Studies by Saleh and Trad, as well by Hashema et al. [38,39], show that, according to the SUPERPAVE and LTPP programs (integrated in the AASHTO M 320 standard), the geographic PG (Performance Grade) predicts the surface temperature of black pavements based on regional climatic conditions. Thus, the determination of the geographic PG is affected not only by climatic data but also by the pavement albedo value, an optical property of the pavement surface nature.

The maximum surface temperatures, shown in Fig. 4a, reached 64 °C for the reference specimen, compared to 61 °C for the TiO_2 -modified specimen. Indicating that the TiO_2 modified pavement will be under lower thermal loads. Consequently, by operating at a lower surface temperature, the TiO_2 -modified sample exhibits a mechanical response to rutting that could match or surpass that of the CA-30 asphalt + conventional fillers. To validate this hypothesis, we quantified the rutting rheological parameters ($G^*/\sin\delta$) at the specific temperatures attained by each sample under real environmental conditions (Table 4), derived from temperature sweeps conducted via DSR rheometer.

The values shown in Table 4 indicate that the specimen incorporating CA-30 + TiO_2 asphalt filler, which has the highest albedo and lowest surface temperature, shows improved rutting resistance under these conditions.

Table 4.

$G^*/\sin\delta$ values obtained with samples, at the surface temperatures reached by the respective specimens under identical solar irradiation conditions.

Sample	$G^*/\sin\delta$	Surface temperature / °C
Asphalt CA-30 + combined fillers	9.1	64
Asphalt CA-30 + TiO ₂ filler	9.9	61

Source: Authors' own work.

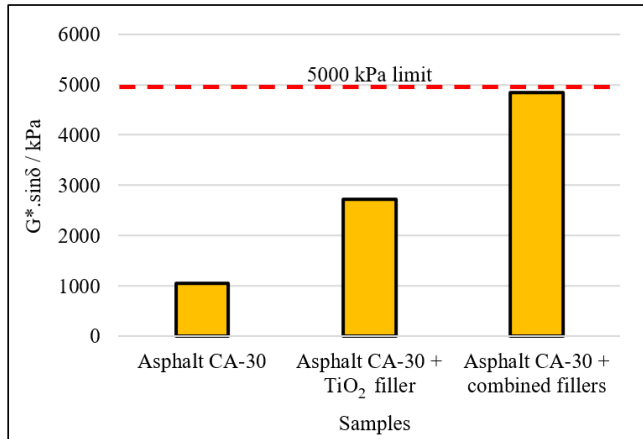


Figure 7. Fatigue parameters obtained at 30°C for the three analyzed samples: a) asphalt CA-30, b) asphalt CA-30 + TiO₂ filler, and c) asphalt CA-30 + combined fillers.

Source: Authors' own work.

3.8 Fatigue damage tolerance

The fatigue parameter $G^* \cdot \sin\delta$ was assessed following the SHRP SUPERPAVE methodology [34], with the limiting value of $G^* \cdot \sin\delta$ defined as 5000 kPa. The values obtained at an intermediate temperature (30°C) for the asphalt CA-30, asphalt CA-30 + combined fillers, and asphalt CA-30 + TiO₂ fillers (shown in Fig. 7) illustrate that the asphalt CA-30 + combined fillers will be the first to fail under fatigue conditions. Therefore, the asphalt CA-30 + TiO₂-filler presents a superior intermediate-temperature performance.

4. Conclusions

It was possible to prepare two different specimens employing CA-30 binder: reference specimen with combined fillers and a modified specimen with TiO₂ filler. To evaluate the physical and rheological properties, samples of the CA-30 asphalt + combined fillers and CA-30 asphalt + TiO₂ fillers were studied. The thermal behaviors of the specimens were also evaluated before and after outdoor exposure for twelve months.

The most relevant conclusions are:

1. **Initial Albedo:** The TiO₂-modified asphalt mixture pavement exhibits a higher initial albedo compared to the reference pavement.
2. **Albedo Increase Over Time:** After 12 months of outdoor exposure, both the reference and TiO₂-modified asphalt pavements showed increased albedo values, with

their coloration becoming lighter compared to the experiment's initial state.

3. **Photocatalytic Effect:** TiO₂ acts as a photocatalyst of a process which explains its more effective bleaching (decolorizing) action.
4. **Thermal Impact Reduction:** The addition of TiO₂ into the asphalt mixture helps to reduce heat transfer from the pavement surface to the surrounding air.
5. **High-Temperature Performance Enhancement:** Although the asphalt CA-30 + combined fillers exhibit the highest rutting resistance, the superior albedo of the asphalt CA-30 + TiO₂ filler specimen, which results in lower surface temperatures under equivalent solar irradiation, enhances the high-temperature performance grade of the latter.
6. **Fatigue Damage Tolerance:** At intermediate temperatures, the asphalt CA-30 + TiO₂ filler exhibits higher fatigue damage tolerance.

References

- [1] Akbari, H., Cartalis, C., Kolokotsa, D., Muscio, A., Pisello, A.L., Rossi, F., Santamouris, M., Synnefa, A., Wong, N.H., and Zinzi, M., Local climate change and urban heat island mitigation techniques – The state of the art. *Journal of Civil Engineering and Management*, 22 (1), pp. 1–16, 2016. DOI: <https://doi.org/10.3846/13923730.2015.1111934>
- [2] Beltran-Hernandez, R.I., Martinez-Ortiz, J.A., Lucho-Constantino, C.A., Lazarraga-Mendiola, L.G., and Bigurra-Alzati, C.A., Alternatives to counteract the effects of anthropogenic soil sealing. *Pädi Boletín Científico de Ciencias Básicas e Ingenierías del ICBI*, [online]. 8(15), art. 115020, 2020. Available at: <https://portal.amelica.org/ameli/journal/595/5953115020/>
- [3] Santamouris, M., Using cool pavements as a mitigation strategy to fight urban heat island. A review of the actual developments. *Renewable and Sustainable Energy Reviews*, 26, pp. 224-240, 2013. DOI: <https://doi.org/10.1016/j.rser.2013.05.047>
- [4] Alchapar, M.L., Correa, E.N., and Cantón, A., Solar reflectance index of pedestrian pavements and their response to aging. *Journal of Clean Energy Technologies*, 1(4), pp. 281-285, 2013. DOI: <https://doi.org/10.7763/JOCET.2013.V1.64>
- [5] Wang, Z., Xie, Y., Mu, M., Feng, L., Xie, N., and Cui, N., Materials to mitigate the urban heat island effect for cool pavement: a brief review. *Buildings*, 12(8), art. 1221, 2022. DOI: <https://doi.org/10.3390/buildings12081221>
- [6] Nwakaire, C., Onn, C.C., Poh, Y.S., Yuen, C.W., and Onodagu, P.D., Urban heat island studies with emphasis on urban pavements: a review. *Sustainable Cities and Society* 63, art. 102476, 2020. DOI: <https://doi.org/10.1016/j.scs.2020.102476>
- [7] Zhu, S., and Mai, X., A review of using reflective pavement materials as mitigation tactics to counter the effects of urban heat island. *Advanced Composites and Hybrid Materials*, [online]. 2(3), pp. 381–388, 2019. Available at: <https://link.springer.com/article/10.1007/s42114-019-00104-9>
- [8] Sophia, K., Souliotis, M., Papaefthimiou, S., Panaras, G., Paravantis, J., Michalena, E., Hills, J., Vouros, A.P., Dymenou, K., and Mihalakakou, G., Cool pavements: state of the art and new technologies. *Sustainability*, 14(9), art. 5159, 2022. DOI: <https://doi.org/10.3390/su14095159>
- [9] Gong, Z., Zhang, L., Wu, J., Xiu, Z., Wang, L., and Miao, Y., Review of regulation techniques of asphalt pavement high temperature for climate change adaptation. *Journal of Infrastructure Preservation and Resilience*, 3, art. 9, 2022. DOI: <https://doi.org/10.1186/s43065-022-00054-5>
- [10] Fernandez-Gomez, W.D., Rondón-Quintana, H.A., and Reytez Liscano, F., A review of asphalt and asphalt mixture aging. *Ingeniería e Investigación*, 33(1), pp. 5-12, 2013. DOI: <https://doi.org/10.15446/ing.investig.v33n1.37659>

- [11] Xie, N., Li, H., Zhang, H., Zhang, X., and Jia, M., Effects of accelerated weathering on the optical characteristics of reflective coatings for cool pavement. *Solar Energy Materials and Solar Cells*, 215, art. 110698, 2020. DOI: <https://doi.org/10.1016/j.solmat.2020.110698>
- [12] Hossain, K., Sertac, A., and Das, P., Effect of ultraviolet aging on rheological properties of asphalt cement. *Proceedings of Canadian Technical Asphalt Association (CTAA)*, 2018.
- [13] Lu, X., Talon, Y., and Redelius, P., Aging of bituminous binders – laboratory tests and field data. *Proceedings of E&E Congress*, 2008.
- [14] Badin, G., Ahmad, N., Ali, H.M., Ahmad, T., and Jameel, M.S., Effect of addition of pigments on thermal characteristics and the resulting performance enhancement of asphalt. *Construction and Building Materials*, 302, art. 124212, 2021. DOI: <https://doi.org/10.1016/j.conbuildmat.2021.124212>
- [15] Ayar, P., Ruhi, A., Baibordy, A., Azadgoleh, M.A., Mohammadi, M.M., and Abdipour, S., Toward sustainable roads: a critical review on nano-TiO₂ application in asphalt pavement. *Innovative Infrastructure Solutions*, 9, art. 148, 2024. DOI: <https://doi.org/10.1007/s41062-024-01450-4>
- [16] Chen, J., Zhou, Z., Wu, J., Hou, S., and Liu, M., Field and laboratory measurement of albedo and heat transfer for pavement materials. *Construction and Building Materials*, 202(4), pp. 46–57, 2019. DOI: <https://doi.org/10.1016/j.conbuildmat.2019.01.028>
- [17] Zhong, Y., Research on thermal reflection and cooling curing coating material of nano modified emulsified asphalt for urban road pavement. *E3S Web of Conferences* 261, art. 02051, 2021. DOI: <https://doi.org/10.1051/e3sconf/202126102051>
- [18] Akbari, H., Levinson, R., and Stern, S., Procedure for measuring the solar reflectance of flat or curved roofing assemblies. *Solar Energy*, 82(7), pp. 648-655, 2008. DOI: <https://doi.org/10.1016/j.solener.2008.01.001>
- [19] ASTM (2006). ASTM E1933-99a: American Society for Testing and Materials, Standard Test Methods for measuring and compensating for emissivity using infrared imaging radiometers. ASTM
- [20] ASTM D5/D5M. Standard Test Method for Penetration of Bituminous Materials, ASTM International, 100 Barr Harbor Drive, West Conshohocken, PA., United States, 2020.
- [21] ASTM D36/D36M. Standard Test Method for Softening Point of Bitumen (Ring-and-Ball Apparatus), ASTM International, 100 Barr Harbor Drive, West Conshohocken, PA., United States, 2020.
- [22] AASHTO M320. Standard Specification for Performance-Grade Asphalt Binder.
- [23] AASHTO T240. Standard Method of Test for Effect of Heat and Air on a Moving Film of Asphalt Binder (Rolling Thin-Film Oven Test).
- [24] Dell'Antonio-Cadorin, N., Staub-de Melo, J.V., Borba-Broering, W., Manfro, A.L., and Salgado-Barra, B., Asphalt nanocomposite with titanium dioxide: Mechanical, rheological and photoactivity performance. *Construction and Building Materials*, 289, art. 123178, 2021. DOI: <https://doi.org/10.1016/j.conbuildmat.2021.123178>
- [25] Villegas-Villegas, R.E., Baldi-Sevilla, A., Aguiar-Moya, J.P., and Loria-Salazar, L., Analysis of asphalt oxidation by means of accelerated testing and environmental conditions. *Transportation Research Record*, 2672(28), pp. 244-255, 2018. DOI: <https://doi.org/10.1177/0361198118777630>
- [26] Ramadhansyah, P.J., Masri, K.A., Norhidayah, A.H., Hainin, M.R., Muhammad Naquiddin, M.W., Haryati, Mohd, K.I., Juraidah, A., Nanoparticle in asphalt binder: a state-of-the-art review. *IOP Conference Series Materials Science and Engineering*, 712, art. 012023, 2020. DOI: <https://doi.org/10.1088/1757-899X/712/1/012023>
- [27] Huang, M. and Wen, X., Experimental study on photocatalytic effect of Nano TiO₂ epoxy emulsified asphalt mixture. *Applied Sciences*, 9(12), art. 2464, 2019. DOI: <https://doi.org/10.3390/app9122464>
- [28] Pasetto, M., Baliello, A., Pasquini, E., and Giacomello, G., High albedo pavement materials. *Eco-efficient Materials for Reducing Cooling Needs in Buildings and Construction*, 2020. DOI: <https://doi.org/10.1016/B978-0-12-820791-8.00002-X>
- [29] Li, H., Harvey, J., and Kendall, A., Field measurement of albedo for different land cover materials and effects on thermal performance. *Building and Environment*, 59, pp. 536–546, 2013. DOI: <https://doi.org/10.1016/j.buildenv.2012.10.014>
- [30] Bentz, D.P., A Computer model to predict the surface temperature and time-of-wetness of concrete pavements and bridge decks building and fire research laboratory. August 2020 National Institute of Standards and Technology Administration, U.S. Department of Commerce.
- [31] Asaeda, T., Vu, C., and Wake, A., Heat storage of pavement and its effect on the lower atmosphere. *Atmospheric Environment*, 30(3), pp. 413-427, 1996. DOI: [https://doi.org/10.1016/1352-2310\(94\)00140-5](https://doi.org/10.1016/1352-2310(94)00140-5)
- [32] Qin, Y., Hiller, J.E., and Meng, D., Linearity between pavement thermophysical properties and surface temperatures. *Journal of Materials in Civil Engineering*, 31(11), art. 2890, 2019. DOI: [https://doi.org/10.1061/\(ASCE\)MT.1943-5533.0002890](https://doi.org/10.1061/(ASCE)MT.1943-5533.0002890)
- [33] Xu, L., Wang, J., Xiao, F., El-Badawy, S., and Awed, A.M. Potential strategies to mitigate the heat island impacts of highway pavement on megacities with considerations of energy uses. *Applied Energy*, 281, art. 116077, 2021. DOI: <https://doi.org/10.1016/j.apenergy.2020.116077>
- [34] Sadeghnejad, M., and Shafabakhsh, G., Use of Nano SiO₂ and Nano TiO₂ to improve the mechanical behaviour of stone mastic asphalt mixtures. *Construction and Building Materials*, 157, pp. 965-974. DOI: <https://doi.org/10.1016/j.conbuildmat.2017.09.163>
- [35] Li, R., Xiao, F., Amirkhanian, S., You, Z., and Huang, J., Developments of nano materials and technologies on asphalt materials—A review. *Construction and Building Materials*, 143, pp. 633-648, 2017. DOI: <https://doi.org/10.1016/j.conbuildmat.2017.03.158>
- [36] Miranda-Argüello, F., Loria-Salazar, L., Aguiar-Moya, J.P., and Leiva-Padilla, P., Measurement of G* in fine asphalt mixes: dynamic mechanical analyzer shear test implementation. *Transportation Research Record*, 2507(1), pp. 39-49, 2019. DOI: <https://doi.org/10.3141/2507-05>
- [37] Mohammed, A.M., and Abed, A., Effect of nano-TiO₂ on physical and rheological properties of asphalt cement. *Open Engineering*, 14(1), art. 20220520, 2024. DOI: <https://doi.org/10.1515/eng-2022-0520>
- [38] Saleh, A.M.M., and Trad, M.A., Generation of asphalt performance grading map for Egypt based on the SUPERPAVETM program. *Construction and Building Materials*, 25, pp. 2248-2253, 2011. DOI: <https://doi.org/10.1016/j.conbuildmat.2010.11.009>
- [39] Abo-Hashema, M.A., Mousa, R.M., Al-Zedjali, S.A., Al Balushi, Q.A., Metwally, M., and Al-Rashdi, M.H., Development of oman performance grade paving map for superpave asphalt mix design. In: *The 19th Annual International Conference on Highway, Airports Pavement Engineering, Infrastructures & Asphalt Technology*. Liverpool, United Kingdom, [online]. 2020. Available at: <https://www.ljmu.ac.uk/%7E/media/files/ljmu/about-us/faculties-and-schools/asphalt-conference/papers/asphalt/asphalt/doi-10,-d-,1515ijpeat20160033.pdf?la=en>

G. Botasso, is PhD in Materials from the National Technological University, BSC. Eng. in Civil Engineer from the National University of Technology, Argentina, and MSc. in Environmental Engineering. Senior Researcher in LEMaC, Center for Road Research of the National University of Technology (Argentina). Secretary of Science Technology and Postgraduate of the National Technological University, La Plata Regional Faculty. He is a teacher in master's and doctoral programs of 10 Master's and Doctoral programs in Latin America. Researcher Category A of the National Technological University. Consultant in road infrastructure program in Argentina, specialized in technology of road materials. Author of more than 80 articles published internationally in specialized magazines and 2 books on asphalt mix technology with the incorporation of recycled rubber. Editor of "Ingenio Tecnológico".
ORCID: 0000-0002-8859-7256

A.M. Castro-Luna, is PhD in Chemistry and Senior Researcher at Scientific Research Commission of the Province of Buenos Aires (CICPBA) Professor of Alternative Energy in the 21st Century, Chemistry Department La Plata Regional Faculty, National Technological University FRLP UTN. She is Director and Co-Director of CICPBA and CONICET Doctoral and Postdoctoral Scholarships and First Director of EnAITecS UTN FRLP (Alternative Energies Technology and Sustainability Group). Areas of Research: Materials Engineering. At present she works in Modified

Pavements, Mitigation of Heat Urban Island, Urban Microclimate and Numerical modeling pavement temperatures.
ORCID: 0000-0003-0799-1313

P. Cabrera, is a BSc. Eng. in Chemical Engineer, PhD. student in Materials Engineering at UTN FRLP and a researcher at LEMaC (Road Research Center) of the National Technological University, Argentina. He obtained a

doctoral scholarship from CONICET with his thesis entitled: "Development and Analysis of Eco-efficient Pavements for the Improvement of Urban Environmental Quality". His work focuses on modified pavements, Urban Heat Island mitigation, urban microclimate and numerical modeling of pavement temperature.

ORCID: 0009-0005-7053-9276